Multifractal detrended cross-correlation analysis for two nonstationary signals

Wei-Xing Zhou (周炜星)*

School of Business, School of Science, Research Center for Econophysics, and Research Center of Systems Engineering, East China University of Science and Technology, Shanghai 200237, China

(Received 19 March 2008; revised manuscript received 19 May 2008; published 18 June 2008)

We propose a method called multifractal detrended cross-correlation analysis to investigate the multifractal behaviors in the power-law cross-correlations between two time series or higher-dimensional quantities recorded simultaneously, which can be applied to diverse complex systems such as turbulence, finance, ecology, physiology, geophysics, and so on. The method is validated with cross-correlated one- and two-dimensional binomial measures and multifractal random walks. As an example, we illustrate the method by analyzing two financial time series.

DOI: 10.1103/PhysRevE.77.066211 PACS number(s): 05.45.Tp, 05.40.−a, 05.45.Df, 89.75.Da

Fractals and multifractals are ubiquitous in natural and social sciences [1]. The most usual records of observable quantities in the real world are in the form of time series and their fractal and multifractal properties have been extensively investigated. There are many methods proposed for this purpose [2,3]. For a single nonstationary time series, a detrended fluctuation analysis (DFA) can be adopted to explore its long-range autocorrelations [4,5] and multifractal features [6]. The DFA method can also be extended to investigate higher-dimensional fractal and multifractal measures [7].

There are many situations where several variables are simultaneously recorded that exhibit long-range dependence or multifractal nature, such as the velocity, temperature, and concentration fields in turbulent flows [8–10], topographic indices and crop yield in agronomy [11,12], and asset prices, indexes, and trading volumes in financial markets [13,14]. Recently, a generalization of the DFA method called detrended cross-correlation analysis (DXA) was proposed to investigate the long-range cross-correlations between two nonstationary time series [15]. Here we show that the DXA method can be generalized to unveil the multifractal features of two cross-correlated signals and higher-dimensional multifractal measures. The validity and potential utility of multifractal detrended cross-correlation analysis (MF-DXA) is illustrated using one- and two-dimensional binomial measures, multifractal random walks (MRWs), and financial prices.

Consider two time series $\{x(i)\}$ and $\{y(i)\}$, where $i=1,2,\ldots,M$. Without loss of generality, we can assume that these two time series have zero means. Each time series is covered with $M_s=(M/s)$ nonoverlapping boxes of size s. The profiles within the vth box, $[l_v+1,l_v+s]$, where $l_v=(v-1)s$, are determined to be $X_v(k)=\sum_{j=1}^{k}x(l_v+j)$ and $Y_v(k)=\sum_{j=1}^{k}y(l_v+j)$, $k=1,\ldots,s$. Assume that the local trends of $\{X_v(k)\}$ and $\{Y_v(k)\}$ are $\{\tilde{X}_v(k)\}$ and $\{\tilde{Y}_v(k)\}$, respectively. There are many different methods for the determination of $\tilde{X}_v$ and $\tilde{Y}_v$. The trend functions could be polynomials [5]. The detrending procedure can also be carried out nonparametrically based on the empirical mode decomposition method [16]. The detrended covariance of each box is calculated as follows:

$$F_v(s)=\frac{1}{s}\sum_{k=1}^{s}[X_v(k)-\tilde{X}_v(k)][Y_v(k)-\tilde{Y}_v(k)]. \quad (1)$$

The qth-order detrended covariance is calculated as

$$F_{xy}(q,s)=\left(\frac{1}{m}\sum_{v=1}^{m}F_v(s)^{q/2}\right)^{1/q} \quad (2)$$

when $q\neq 0$ and

$$F_{xy}(0,s)=\exp\left(\frac{1}{2m}\sum_{v=1}^{m}\ln F_v(s)\right). \quad (3)$$

We then expect the following scaling relation:

$$F_{xy}(q,s)\sim s^{h_{xy}(q)}. \quad (4)$$

When $X=Y$, the above method reduces to the classic multifractal DFA.

In order to test the validity of the power-law behavior in Eq. (4), we construct two binomial measures from the p model with known analytic multifractal properties as a first example [17]. Each multifractal signal is obtained in an iterative way. We start with the zeroth iteration $g=0$, where the data set $z(i)$ consists of one value $z^{(0)}(1)=1$. In the gth iteration, the data set $\{z^{(g)}(i): i=1,2,\ldots,2^g\}$ is obtained from $z^{(g)}(2k+1)=pz^{(g-1)}(2k+1)$ and $z^{(g)}(2k)=(1-p)z^{(g-1)}(2k)$ for $k=1,2,\ldots,2^{g-1}$. When $g\rightarrow\infty$, $z^{(g)}(i)$ approaches a binomial measure, whose scaling exponent function $H_{zz}(q)$ has an analytic form [17,18],

$$H_{zz}(q)=1/q-\log_2[p^q+(1-p)^q]/q. \quad (5)$$

In our simulation, we have performed $g=17$ iterations with $p=p_x=0.3$ for $x(i)$ and $p=p_y=0.4$ for $y(i)$. The analytic scaling exponent functions $H_{xx}(q)$ and $H_{yy}(q)$ of x and y are expressed in Eq. (5). The cross-correlation coefficient is 0.82. We find that F_{xy}, F_{xx}, and F_{yy} all scale with respect to s as power laws. Note that there are evident log-periodic oscillations decorating the power laws, which is an inherent feature of the constructed binomial measures [19]. The best estimates of the power-law exponents are obtained when s is sampled log-periodically [20]. The resultant power-law exponents h_{xy}, h_{xx}, and h_{yy} are illustrated in Fig. 1. The MF-

*wxzhou@ecust.edu.cn

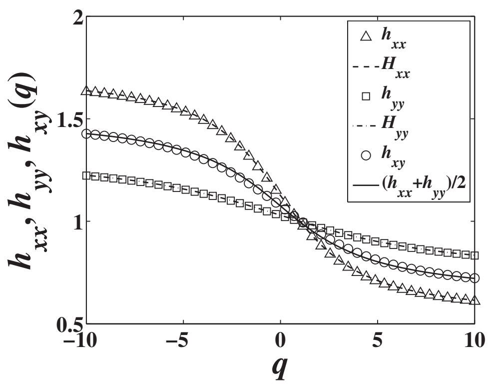

FIG. 1. Scaling exponents $h_{xy}(q)$ estimated using the multifractal detrended cross-correlation analysis of two cross-correlated binomial measures generated from the p model. The numerically estimated exponents $h_{xx}(q)$ and $h_{yy}(q)$ obtained from the multifractal detrended fluctuation analysis of $x(i)$ and $y(i)$ are also presented, and well match the analytical curves $H_{xx}(q)$ and $H_{yy}(q)$. This example illustrates the relation $h_{xy}(q)=[h_{xx}(q)+h_{yy}(q)]/2$.

DFA analysis gives $h_{xx}(q)=H_{xx}(q)$ and $h_{yy}(q)=H_{yy}(q)$. We also find that

$$h_{xy}(q) = [h_{xx}(q) + h_{yy}(q)]/2. \tag{6}$$

For monofractal autoregressive fractional moving average (ARFIMA) signals, this relation with $q=2$ is also observed [15].

As a second example, we consider multifractal random walks [21]. The increments of a MRW are $\epsilon(k)e^{\omega(k)}$, where $\epsilon(k)$ and $\omega(k)$ are uncorrelated and $\omega(k)$ is a white noise. In order to generated two cross-correlated MRWs, we can generate two time series ϵ_x and ϵ_y possessing the properties in the MRW framework and rearrange ϵ_y such that the rearranged series ϵ_y has the same rank ordering as ϵ_x [22]. We generate two MRW signals of size 2^{16} with $\lambda^2=0.02$ for $x(i)$ and $\lambda^2=0.04$ for $y(i)$, whose cross-correlation coefficient is 0.69. When q is negative, no evident power-law scaling is observed for $F_{xy}(s)$, which has great fluctuations. When q is positive, nice power-law scaling is observed for F_{xy}, F_{xx}, and F_{yy}, as illustrated in Fig. 2(a) for $q=2$ and 5. The power-law exponents h_{xy}, h_{xx}, and h_{yy} are illustrated in Fig. 2(b). We see that Eq. (6) holds in repeated numerical experiments. However, this relation does not hold for some other realizations of MRWs.

We now apply the MF-DXA method to the daily closing prices of the Dow Jones Industrial Average (DJIA) and National Association of Securities Dealers Automated Quotation (NASDAQ) indices. For comparison, we have used the same data sets and same scaling range as in Ref. [15]. No evident power-law scaling is observed for negative q values. For positive q, we see power-law dependence of F_{xy}, F_{xx}, and F_{yy} against time lag s. Two examples are illustrated in Fig. 3(a) for $q=2$ and 5, where the case of $q=2$ reproduces the results in Ref. [15]. The power-law exponents h_{xy}, h_{xx}, and h_{yy} are depicted in Fig. 2(b); they are nonlinear functions with respect to q. We see that each time series of the absolute returns possesses multifractal nature and their power-law cross-correlations also exhibit a multifractal nature.

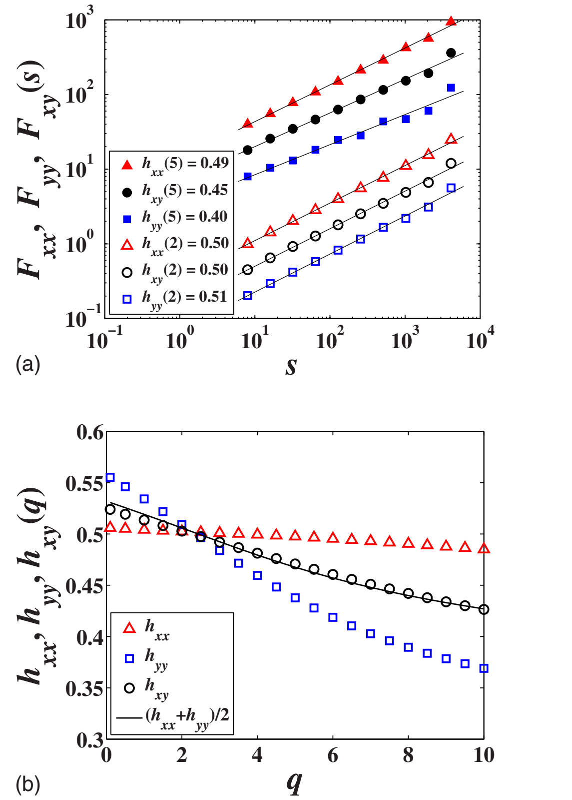

FIG. 2. (Color online) Multifractal nature of the power-law cross correlations of two MRWs. (a) Power-law scaling in F_{xy}, F_{xx}, and F_{yy} with respect to s for $q=2$ and 5; (b) power-law exponents h_{xy}, h_{xx}, and h_{yy}.

We can generalize the one-dimensional (1D) MF-DFA to the 2D version and its extension to higher dimensions is straightforward. Consider two self-similar (or self-affine) surfaces of identical sizes, which can be denoted by two arrays $x(i,j)$ and $y(i,j)$, where $i=1,2,\ldots,M$ and $j=1,2,\ldots,N$. The surfaces are partitioned into $M_s \times N_s$ disjoint square segments of the same size $s \times s$, where $M_s=(M/s)$ and $N_s=(N/s)$. Each segment can be denoted by $x_{v,w}$ or $y_{v,w}$ such that $x_{v,w}(i,j)=x(l_v+i,l_w+j)$ and $y_{v,w}(i,j)=y(l_v+i,l_w+j)$ for $1 \le i,j \le s$, where $l_v=(v-1)s$ and $l_w=(w-1)s$.

For each segment $x_{v,w}$ identified by v and w, the cumulative sum $X_{v,w}(i,j)$ is calculated as follows:

$$X_{v,w}(i,j) = \sum_{k_1=1}^{i} \sum_{k_2=1}^{j} x_{v,w}(k_1,k_2), \tag{7}$$

where $1 \le i,j \le s$. The cumulative sum $Y_{v,w}(i,j)$ can be calculated similarly from $y_{v,w}$. The detrended covariance of the two segments can be determined as follows:

$$F_{v,w}(s) = \frac{1}{s^2} \sum_{i=1}^{s} \sum_{j=1}^{s} [X_{v,w}(i,j) - \widetilde{X}_{v,w}(i,j)][Y_{v,w}(i,j) - \widetilde{Y}_{v,w}(i,j)], \tag{8}$$

where $\widetilde{X}_{v,w}$ and $\widetilde{Y}_{v,w}$ are the local trends of $X_{v,w}$ and $Y_{v,w}$, respectively. The trend function is prechosen in different

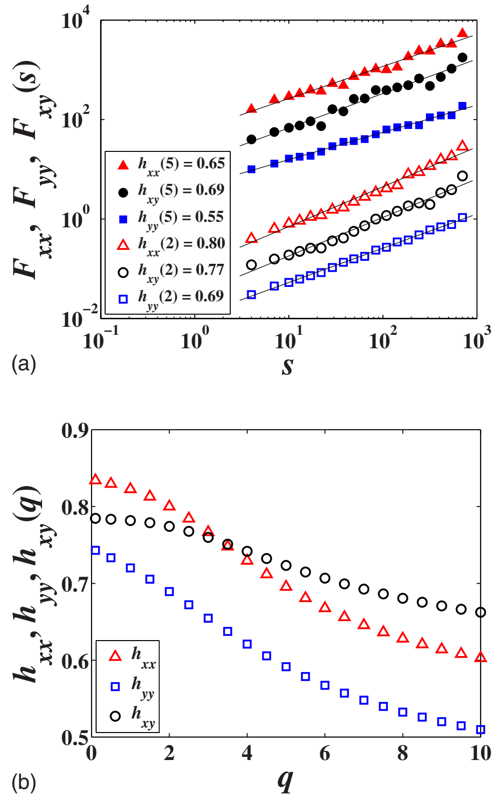

FIG. 3. (Color online) Multifractal nature of the power-law cross correlations of the absolute values of daily price changes for DJIA and NASDAQ indices in the period from July 1993 to November 2003. (a) Power-law scaling in F_{xy}, F_{xx}, and F_{yy} with respect to s for $q=2$ and 5. The scaling range is the same as in Ref. [15]. (b) Dependence of the power-law exponents h_{xy}, h_{xx}, and h_{yy} as nonlinear functions of q, indicating the presence of multifractality. There is no clear relation between these exponents.

function forms [7]. The simplest function could be a plane $\tilde{u}(i,j)=ai+bj+c$, which is adopted to test the validation of the method. The overall detrended cross correlation is calculated by averaging over all the segments, that is,

$$F_{xy}(q,s)=\left(\frac{1}{M_sN_s}\sum_{v=1}^{M_s}\sum_{w=1}^{N_s}[F_{v,w}(s)]^{q/2}\right)^{1/q}, \tag{9}$$

where q can take any real value except for $q=0$. When $q=0$, we have

$$F_{xy}(q,s)=\exp\left(\frac{1}{2M_sN_s}\sum_{v=1}^{M_s}\sum_{w=1}^{N_s}\ln[F_{v,w}(s)]\right), \tag{10}$$

according to L'Hôpital's rule. The scaling relation between the detrended fluctuation function $F_{xy}(q,s)$ and the size scale s can be determined as

$$F_{xy}(q,s)\sim s^{h_{xy}(q)}. \tag{11}$$

Since N and M need not be multiples of the segment size s, two orthogonal strips at the end of the profile may remain. Taking these ending parts of the surface into consideration, the same partitioning procedure can be repeated starting from the other three corners [23].

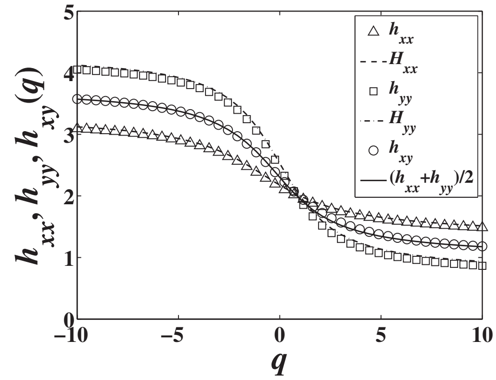

FIG. 4. Multifractal detrended cross-correlation analysis of two cross-correlated synthetic binomial measures from the p model. The size of each multifractal is 4096×4096 and the cross-correlation coefficient is 0.48. The numerical exponents $h_{xx}(q)$ and $h_{yy}(q)$ obtained from the multifractal detrended fluctuation analysis of X and Y are located approximately on the analytical curves $H_{xx}(q)$ and $H_{yy}(q)$. This example illustrates the relation $h_{xy}(q)=[h_{xx}(q)+h_{yy}(q)]/2$.

It is worth pointing out that the order of cumulative summation and partitioning is crucial in the analysis of two- or higher-dimensional multifractals. Consider the point located at (l_v+i,l_w+j) in the box identified by v and w, where $1\le i,j\le s$. The cumulative sum $X(l_v+i,l_w+j)$ can be expressed as follows:

$$X(l_v+i,l_w+j)=X_{v,w}(i,j)+\sum_{k_1=1}^{l_v}\sum_{k_2=1}^{l_w}x(k_1,k_2)+\sum_{k_1=1}^{l_v}\sum_{k_2=l_w}^{l_w+j}x(k_1,k_2)+\sum_{k_1=l_v}^{l_v+i}\sum_{k_2=1}^{l_w}x(k_1,k_2). \tag{12}$$

For any pair of (i,j), $X_{v,w}(i,j)$ is localized within the segment $x_{v,w}$, while $X(l_v+i,l_w+j)$ contains extra information outside the segment as shown above, which is not constant for different i and j and thus cannot be removed by the detrending procedure. We find that the power-law scaling is absent if $X(l_v+i,l_w+j)$ is used in Eq. (7). This observation is analogous to the case of higher-dimensional detrended fluctuation analysis [7].

We now present numerical experiments validating the two-dimensional multifractal detrended cross-correlation analysis. There exist several methods for the synthesis of two-dimensional multifractal measures or multifractal rough surfaces [24]. The most usual method follows a multiplicative cascading process, which can be either deterministic or stochastic [17,25–27]. The simplest one is the p model, proposed to mimic the kinetic energy dissipation field in fully developed turbulence [17]. Starting from a square, one partitions it into four subsquares of the same size and assigns four given proportions of measure p_{11}, p_{12}, p_{21}, and p_{22} to them. Then each subsquare is divided into four smaller squares and the measure is redistributed in the same way. This procedure is repeated g times, and we generate multifractal "surfaces" of size $2^g\times2^g$. The analytical expression of $H_{xx}(q)$ or $H_{yy}(q)$ for individual multifractals has the same form,

$$H_{zz}(q) = [2 - \log_2(p_{11}^q + p_{12}^q + p_{21}^q + p_{22}^q)]/q, \qquad (13)$$

where the subscript $z=x$ for X and $z=y$ for X.

In our simulation, we have used $p_{11}=0.10$, $p_{12}=0.20$, $p_{21}=0.30$, and $p_{22}=0.40$ for X and $p_{11}=0.05$, $p_{12}=0.15$, $p_{21}=0.20$, and $p_{22}=0.60$ for Y. We find that the cross-correlation coefficient between the two multifractals depends linearly on the generation number g, $c=-0.0408g+0.9528$, where the value of R^2 is 0.9997. The 95% confidence intervals for the slope and intercept are $[-0.0415,-0.0402]$ and $[0.9489,0.9566]$, respectively. In our numerical experiment, we have used $g=12$, which gives $c=0.48$. Very nice power-law behaviors are confirmed in $F_{xy}(q,s)$, $F_{xx}(q,s)$, and $F_{yy}(q,s)$ with respect to s for different values of q. The resultant power-law exponents $h_{xy}(q)$, $h_{xx}(q)$, and $h_{yy}(q)$ are illustrated in Fig. 4, marked with open circles, squares, and triangles, respectively. We find that the relation $h_{xy}(q)=[h_{xx}(q)+h_{yy}(q)]/2$ holds.

In summary, we have proposed a multifractal detrended cross-correlation analysis to explore the multifractal behaviors in power-law cross-correlations between two simultaneously recorded time series or higher-dimensional signals. The MF-DXA method is a combination of multifractal analysis and detrended cross-correlation analysis. Potential fields of application include turbulence, financial markets, ecology, physiology, geophysics, and so on.

We thank J.-F. Muzy for help in generating two cross-correlated MRWs and G.-F. Gu for discussions. This work was partly supported by NSFC (Grant No. 70501011), Fok Ying Tong Education Foundation (Grant No. 101086), Shanghai Rising-Star Program (Grant No. 06QA14015), and Program for New Century Excellent Talents in University (Grant No. NCET-07-0288).

[1] B. B. Mandelbrot, *The Fractal Geometry of Nature* (W. H. Freeman, New York, 1983).

[2] M. Taqqu, V. Teverovsky, and W. Willinger, Fractals **3**, 785 (1995).

[3] A. Montanari, M. S. Taqqu, and V. Teverovsky, Math. Comput. Modell. **29**, 217 (1999).

[4] C.-K. Peng, S. V. Buldyrev, S. Havlin, M. Simons, H. E. Stanley, and A. L. Goldberger, Phys. Rev. E **49**, 1685 (1994).

[5] K. Hu, P. C. Ivanov, Z. Chen, P. Carpena, and H. E. Stanley, Phys. Rev. E **64**, 011114 (2001).

[6] J. W. Kantelhardt, S. A. Zschiegner, E. Koscielny-Bunde, S. Havlin, A. Bunde, and H. E. Stanley, Physica A **316**, 87 (2002).

[7] G.-F. Gu and W.-X. Zhou, Phys. Rev. E **74**, 061104 (2006).

[8] C. Meneveau, K. R. Sreenivasan, P. Kailasnath, and M. S. Fan, Phys. Rev. A **41**, 894 (1990).

[9] F. Schmitt, D. Schertzer, S. Lovejoy, and Y. Brunet, Europhys. Lett. **34**, 195 (1996).

[10] S. Beaulac and L. Mydlarski, Phys. Fluids **16**, 2126 (2004).

[11] A. N. Kravchenko, D. G. Bullock, and C. W. Boast, Agron. J. **92**, 1279 (2000).

[12] T. B. Zeleke and B.-C. Si, Agron. J. **96**, 1082 (2004).

[13] K. Ivanova and M. Ausloos, Eur. Phys. J. B **8**, 665 (1999).

[14] K. Matia, Y. Ashkenazy, and H. E. Stanley, Europhys. Lett. **61**, 422 (2003).

[15] B. Podobnik and H. E. Stanley, Phys. Rev. Lett. **100**, 084102 (2008).

[16] Z.-H. Wu, N.-E. Huang, S. R. Long, and C.-K. Peng, Proc. Natl. Acad. Sci. U.S.A. **104**, 14889 (2007).

[17] C. Meneveau and K. R. Sreenivasan, Phys. Rev. Lett. **59**, 1424 (1987).

[18] T. C. Halsey, M. H. Jensen, L. P. Kadanoff, I. Procaccia, and B. I. Shraiman, Phys. Rev. A **33**, 1141 (1986).

[19] D. Sornette, Phys. Rep. **297**, 239 (1998).

[20] W.-X. Zhou, Z.-Q. Jiang, and D. Sornette, Physica A **375**, 741 (2007).

[21] E. Bacry, J. Delour, and J.-F. Muzy, Phys. Rev. E **64**, 026103 (2001).

[22] M. I. Bogachev, J. F. Eichner, and A. Bunde, Phys. Rev. Lett. **99**, 240601 (2007).

[23] J. W. Kantelhardt, E. Koscielny-Bunde, H. H. A. Rego, S. Havlin, and A. Bunde, Physica A **295**, 441 (2001).

[24] N. Decoster, S. G. Roux, and A. Arnéodo, Eur. Phys. J. B **15**, 739 (2000).

[25] B. B. Mandelbrot, J. Fluid Mech. **62**, 331 (1974).

[26] E. A. Novikov, Phys. Fluids A **2**, 814 (1990).

[27] C. Meneveau and K. R. Sreenivasan, J. Fluid Mech. **224**, 429 (1991).